Increasing the Fuel Economy of Connected and Autonomous Lithium-Ion Electrified Vehicles

Zachary D. Asher, David A. Trinko and Thomas H. Bradley

Abstract When the sensors and signals that enable connected and autonomous vehicle (CAV) technology are combined with vehicle electrification, new vehicle control strategies that improve fuel economy (FE) are possible through perception, planning, and a control request issued to the vehicle plant. In this chapter, each CAV technology that could contribute to planning is introduced and discussed. Next, the techniques for modeling and validating a vehicle plant and running controller are discussed. Then, three planning-based control strategies are developed: (1) an Optimal Energy Management Strategy (Optimal EMS), (2) Eco-Driving strategies, and (3) an Optimal EMS combined with Eco-Driving strategies. Each of these planning-based control strategies is evaluated using a validated model of a 2010 Toyota Prius in Autonomie so that engine power, battery state of charge, and FE results can be compared. The results indicate that a 40% + FE improvement is possible when an Optimal EMS is combined with Eco-Driving for city drive cycles. Overall, as more vehicles incorporate CAV technologies and electrification, these FE improvements will be easier to achieve and will have a greater impact on transportation sustainability.

1 Introduction

Modern vehicles are incorporating electrification to evolve from conventional vehicles (CVs) to hybrid electric vehicles (HEVs), plug-in hybrid electric vehicles (PHEVs), and fully electric vehicles (EVs) [1, 2]. At the same time, rapid advances

Z. D. Asher · D. A. Trinko · T. H. Bradley (✉)
Department of Mechanical Engineering, Colorado State University,
Fort Collins, CO 80524, USA
e-mail: Thomas.Bradley@ColoState.edu

Z. D. Asher
e-mail: asherzd@gmail.com

D. A. Trinko
e-mail: david.trinko@gmail.com

G. Pistoia and B. Liaw (eds.), *Behaviour of Lithium-Ion Batteries in Electric Vehicles*, Green Energy and Technology,
https://doi.org/10.1007/978-3-319-69950-9_6

in computational technology have provided vehicles with the ability to perceive their environment by use of sensor technologies and computer systems [3]. Combined, these two trends provide new possibilities for improving fuel economy (FE) from vehicle control.

Connected and Autonomous Vehicle Technology

Connected and autonomous vehicle (CAV) technology can be realized using sensors and signals currently available, but can be made more efficient and reliable using near-future sensors and signals. Currently available CAV technology includes camera systems (CS), radio detection and ranging (RaDAR), light detection and ranging (LiDAR), the global positioning system (GPS), and drive cycle databases. Near-future CAV technology includes an advanced global navigation satellite systems (GNSS), vehicle-to-vehicle communication (V2V), vehicle-to-infrastructure communication (V2I), and vehicle-to-everything communication (V2X). Each of these sensors and signals is discussed in Sect. 2 and each contributes to the new trend of vehicle sensing which can be leveraged in electrified vehicles to improve FE.

Lithium-Ion Vehicle Electrification

Vehicle electrification has facilitated new vehicle configurations, architectures, and control strategies. Additionally, lithium-ion vehicle batteries have provided improved battery capacity allowing increased vehicle powertrain operational freedom [4]. Hybrid vehicles such as HEVs and PHEVs provide the most freedom in vehicle powertrain control due to the two sources of propulsive power that can be used.

New Possibilities for Improving Fuel Economy

When CAV technology is combined with lithium-ion vehicle electrification, new FE improvement control strategies are possible. CAV technology enables vehicle environment perception, also known as a worldview, and consequently a prediction of future vehicle operation. This vehicle operation prediction can be leveraged by a planning algorithm to compute a vehicle control strategy to improve FE. This control strategy is issued as a request to the vehicle running controller, which implements the control request without violating operational constraints in the vehicle plant. The energy consumption from the vehicle can then be measured. A systems-level viewpoint of this process is shown in Fig. 1.

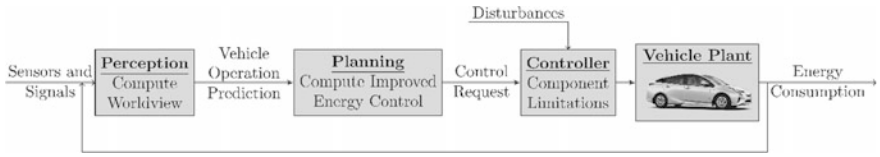

Fig. 1 A systems-level viewpoint presenting the subsystems required for advanced control strategies enabled by connected and autonomous technology

Improved vehicle powertrain operation, referred to as an Optimal Energy Management Strategy (Optimal EMS), is achieved by increasing the efficiency of the vehicle powertrain without modification of the drive cycle. Improved vehicle operation, referred to as Eco-Driving, is achieved by decreasing the energy output of the vehicle through modification of the drive cycle. Both of these strategies are enabled by CAV technologies, and their FE improvements are significant due to the powertrain flexibility of electrified vehicles.

2 Perception Enabled by Connected and Autonomous Vehicle Technology

CAV technologies such as CS, RaDAR, LiDAR, GPS, GNSS, drive cycle databases, V2V, V2I, and V2X enable perception of the vehicle environment, or worldview, which can be leveraged to predict vehicle routes, vehicle speeds, energy use, and driver behavior, thus enabling the FE improvement techniques of an Optimal EMS and Eco-Driving.

Currently available CAV technology that could be used to implement an Optimal EMS and Eco-Driving is shown in Fig. 2 and discussed in Table 1. Near-future CAV technology that could be used to implement an Optimal EMS and Eco-Driving is shown in Fig. 3 and discussed in Table 2. Utilization of only currently available CAV technology to improve FE through an Optimal EMS and/or Eco-Driving is a frequently debated topic in the literature, and ongoing efforts are an active subject of research [5]. But, the literature is consistent in the view that when near-future CAV technology is available, significant FE improvements through an Optimal EMS and Eco-Driving will be feasible. Note that the Optimal EMS and Eco-Driving FE impacts shown in Tables 1 and 2 are highly dependent on the vehicle type, architecture, and the drive cycle.

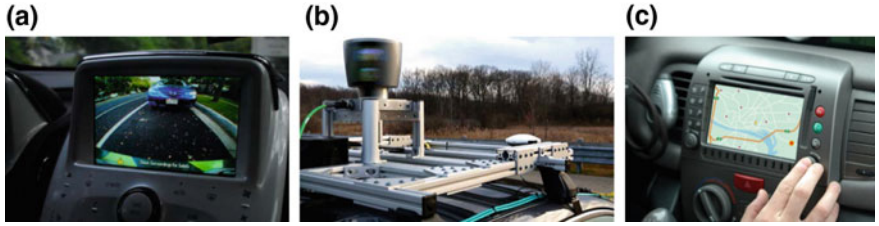

Fig. 2 Vehicle implementation of currently available CAV technologies: **a** CS, **b** LiDAR [6], and **c** GPS [7]

Table 1 Currently available CAV technologies and their potential usage with Eco-Driving and Optimal EMS FE improvement techniques

CAV technology	Eco-Driving impacts	Optimal EMS impacts	FE impact
Camera systems (CS)	Localized velocity modification helps enable adaptive cruise control	Localized prediction of future velocity through sign recognition	Small FE improvements from short predictions
Radio detection and ranging (RaDAR)	Localized velocity modification fully enables adaptive cruise control	Localized prediction of future velocity through object recognition	Small FE improvements on the highway
Light detection and ranging (LiDAR)	Higher accuracy localized velocity modification which could enable lane switching	Higher accuracy localized prediction of future velocity through object recognition	Better FE improvements on the highway
Global positioning system (GPS)	Velocity modification to coincide with speed limits along the route	Basic prediction of the full drive cycle using stop light and speed limit information	Prediction accuracy-dependent FE improvements along an entire route
Drive cycle database	Velocity modifications in historically costly sections of the drive cycle	Route length velocity predictions that improve with repeated trips	Prediction accuracy-dependent FE improvements along an entire route

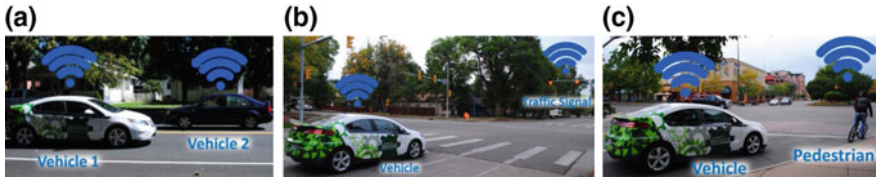

Fig. 3 Conceptual examples of near-future CAV technologies: **a** V2V, **b** V2I, and **c** V2X

2.1 Camera Systems

CS were one of the first steps taken to increase vehicle environment awareness, enabling monitoring of other, less aware vehicles. CS can interpret immediate vehicle surroundings to provide a localized prediction of vehicle speed. They can recognize other vehicle locations [8], obstructions [9], traffic signs [10], and traffic signals [11], thus determining the driving vehicle's likely speeds in the next few seconds. This information can be used to increase FE through Eco-Driving [12, 13] and using an Optimal EMS. CS are currently in use by modern vehicles most commonly for backup assistance (shown in Fig. 2a), collision safety [14–17], and adaptive cruise control [18] which becomes more accurate and reliable when combined with RaDAR or LiDAR (as shown in Fig. 2b) sensors as discussed in Sect. 2.2.

Table 2 Near-future CAV technologies and their potential usage with Eco-Driving and Optimal EMS FE improvement techniques

CAV Technology	Eco-Driving impacts	Optimal EMS impacts	FE impact
Global navigation satellite systems (GNSS)	Velocity modification to coincide with speed limits along the route	Route length velocity predictions that improve with repeated trips	Prediction accuracy-dependent FE improvements along an entire route
Vehicle-to-vehicle comm. (V2V)	Opens numerous driving velocity modifications and enables cooperative adaptive cruise control	High accuracy of future velocity prediction along a busy road	Large FE improvements along busy roads
Vehicle-to-infrastructure comm. (V2I)	Enables velocity modifications along an entire route that coordinate with traffic signals	High accuracy of future velocity prediction near traffic lights	Large FE improvements near traffic lights
Vehicle-to-everything comm. (V2X)	Enables full velocity modification along an entire route while accounting for all drive cycle obstructions	High accuracy of future velocity prediction along the full route	Enables absolute optimal FE

2.2 Radio/Light Detection and Ranging

RaDAR is an inexpensive means of determining additional vehicle environment information and monitoring other, less aware vehicles. RaDAR and LiDAR provide similar information to CS about vehicle surroundings, but they interpret the vehicle surroundings differently. Comparing the transmitted and received radio waves (RaDAR) or light waves (LiDAR) provides advantages such as good performance in low visibility and disadvantages such as the inability to interpret street signs [19, 20]. The most robust localized prediction of vehicle driving speed can be obtained with the combination of RaDAR/LiDAR and CS [21–23], leading to improved FE increases from Eco-Driving [24, 25] and adaptive cruise control [26, 27].

2.3 Global Navigation Satellite Systems

In order to expand beyond immediate vehicle surroundings, information from GNSS can be used. GNSS technologies allow advanced knowledge of the vehicle

route (and thus the speed limits along the route) and the current location of the vehicle along the route. This information can be leveraged to determine vehicle velocities that meet the speed limit but improve FE through Eco-Driving [28, 29]. Even though GNSS cannot predict traffic lights and sudden accidents, GNSS provides sufficient information for Optimal EMS FE improvements [30, 31].

The United States' GPS is an example of a GNSS and has already been successfully integrated into modern vehicles, as shown in Fig. 2c, for route calculations and traffic warnings. Current GPS technology requires improvements to identify vehicle orientation, velocity, and position in all environments [32–34], but upcoming GNSS technologies allow improved frequency and accuracy in determining these vehicle parameters [35–37].

2.4 Drive Cycle Databases

A database of previous drive cycles can improve autonomous navigation [38] and is particularly valuable when implementing an Optimal EMS. Polling a drive cycle database for the same drive cycle is unique because it provides a detailed velocity prediction for the entire drive cycle. But, for previously undriven drive cycles, there is no drive cycle database to poll and thus alternative perception methods are required. FE improvements can be realized by through Eco-Driving and an Optimal EMS [30, 31, 39, 40] when a drive cycle database is used in conjunction with the current vehicle state.

2.5 Vehicle-to-Vehicle Communications

Information gained from CS, RaDAR/LiDAR, drive cycle databases, and GNSS on one vehicle can be communicated to other vehicles wirelessly through V2V and is anticipated to occur over the DSRC 5.85–5.925 GHz band [41]. Direct knowledge of other vehicle information increases prediction accuracy when used with CS, RaDAR, and GNSS information for high FE gains from Eco-Driving [42, 43] and an Optimal EMS [44]. A special case of Eco-Driving, which is enabled by V2V communication, is known as "platooning" where multiple vehicles drive very close together to minimize air drag [45].

2.6 Vehicle-to-Infrastructure Communications

Advanced communication of traffic signal state can facilitate FE-improved vehicle drive cycles as well as powertrain control. Vehicles with advanced warnings of traffic lights can improve FE through Eco-Driving by maintaining more consistent

vehicle speeds and planning efficient accelerations/decelerations [46–49]. Initial research demonstrates that significant FE improvements from an Optimal EMS are also possible once V2I has been implemented [39, 44, 50, 51].

2.7 Vehicle-to-Everything Communications

V2X involves communication with pedestrians (V2P), mobile devices (V2D), the cloud (V2C), and the grid (V2G). Despite being several decades away from real-world realization, near-perfect drive cycle prediction enabled by this technology would maximize FE gains from Eco-Driving [52–59] and an Optimal EMS.

3 Vehicle Plant and Controller Model

Real-world feasibility of perception and planning FE improvement control strategies must be investigated using high-fidelity models. These models can be validated by comparing the simulated vehicle parameters (such as engine power, battery state of charge (SOC), fuel consumption) with real-world vehicle parameters over the same drive cycle. When comparing the simulated FE to the real-world FE for a variety of fixed drive cycles, it is desirable to obtain a difference of no more than 3% across all drive cycles [60, 61].

There are several options for obtaining a high-fidelity model. The Autonomie software developed at Argonne National Labs is comprehensive and popular and can be interfaced with MATLAB through Simulink. Alternatively, the Future Automotive Systems Technology Simulator (FASTSim) developed by the National Renewable Energy Lab is less comprehensive but allows for faster simulations when considering vehicle fleets. Another option is to create a custom model using advanced modeling software, e.g., Modelica.

The Autonomie simulation tool has demonstrated close alignment with real-world Chevrolet Volt PHEV operation [60] and Toyota Prius HEV operation [61], thus demonstrating the model's effectiveness. The drawback of using Autonomie is that the specific vehicle model parameters used in those studies are not publically available and customers must manually override the preloaded vehicle models. To obtain a validated vehicle model, numerous parameters such as control logic, engine operation maps, and component efficiency maps must be modified.

An alternative method is to develop a custom high-fidelity vehicle model using the Modelica modeling language. Modelica is a free tool that uses a differential algebraic equation solver to simulate real-world stimulus responses and can be used in a wide variety of applications to develop models of desired fidelity [62–64]. This custom simulation tool is useful because modifications for FE improvement strategies are clear and transparent in comparison with Autonomie. The drawback

of this simulation technique is that Modelica does not receive as much support, resulting in program crashes and arduous troubleshooting.

The first step in the analysis of improved FE control strategies is to establish a Baseline Energy Management Strategy (Baseline EMS) that mimics existing vehicle operation. This Baseline EMS should be validated against physical vehicle operation characteristics such as engine power, battery SOC, and FE over a variety of drive cycles (city, highway, aggressive, etc.). Typically, the city-focused Urban Dynamometer Driving Schedule (UDDS), the highway-focused Highway Fuel Economy Test (HWFET), and the aggressive US06 drive cycles are used, while the New York City Cycle (NYCC) can also be added. These drive cycles are shown in Fig. 4. They are used to validate the model and investigate alternate planning methods in Sects. 4–6. A 2012 Toyota Prius PHEV Autonomie model validation is shown in Table 3. Because the Baseline EMS is in close agreement with physically measured values, the model is considered validated.

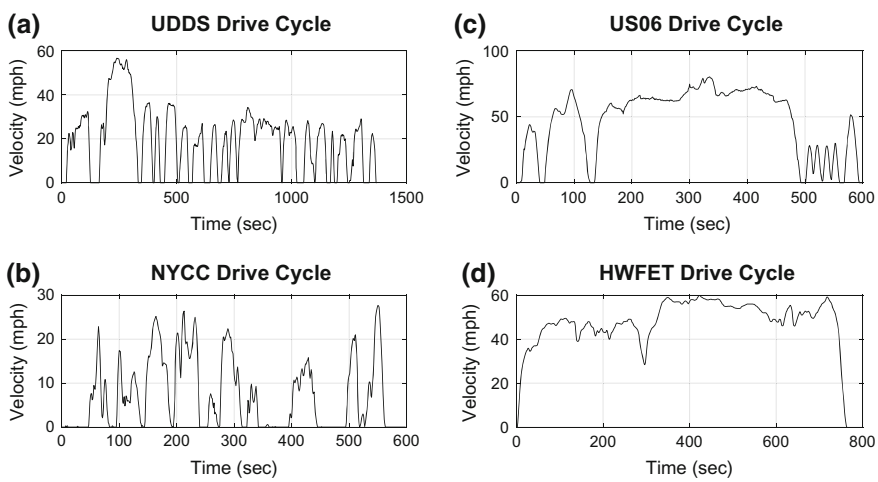

Fig. 4 Four US drive cycles frequently used by the Environmental Protection Agency (EPA)

Table 3 Simulated and measured FE and battery energy usage comparison for a 2012 Toyota Prius PHEV model developed using Autonomie

EPA drive cycle	Simulated fuel economy (mpg)	Measured fuel economy [65] (mpg)	Percent diff. (%)	Simulated battery net energy (Wh)	Measured battery net energy [65] (Wh)	Percent diff. (%)
UDDS	79.3	81.5	2.8	366.2	237.6	35.1
HWFET	86.5	88.8	2.7	582.2	549.0	5.7
US06	53.4	54.3	1.7	450.2	472.7	5.0

4 Planning Method 1: An Optimal Energy Management Strategy

An Optimal EMS enables FE improvements by increasing powertrain efficiency along a fixed drive cycle. Methods used to determine the global Optimal EMS include dynamic programming (DP) [66, 67] and Pontryagin's Minimization Principle (PMP), which is based on calculus of variations [68, 69]. Note that alternate Optimal EMS exists that makes optimality trade-offs to improve robustness such as stochastic dynamic programming (SDP) [70] and adaptive equivalent consumption minimization strategy (a-ECMS) [71] as well as Optimal EMS that makes optimality trade-offs for computation time such as optimized rule-based control [72], equivalent consumption minimization strategy (ECMS) [73], and model predictive control (MPC) [74]. Despite the numerous Optimal EMS derivation strategies, DP remains the overwhelming favorite due to its ease of use, robustness, and lack of dependence on derivatives or analytic expressions [75].

4.1 Deriving the Optimal EMS

DP finds the optimal solution using backward recursion, which avoids solutions that are not optimal as defined by the Bellman principle of optimality [67]. For every feasible state variable value, the optimal solution is stored. The globally optimal control is derived using the standard DP formulation of

$$\text{Dynamic Equation}: S(k+1) = S(k) + f(S, u, w, k)\,\Delta t \tag{1}$$

$$\text{Cost Function}: J = \sum_{k=0}^{N-1} f(S, u, w, k, \Delta t) \tag{2}$$

$$\text{State Feasibility Constraints}: S_{\min} \le S(k) \le S_{\max} \quad (k = 0, \ldots N) \tag{3}$$

$$\text{Control Feasibility Constraints}: u_{\min} \le u(k) \le u_{\max} \quad (k = 0, \ldots N-1) \tag{4}$$

where S is the state, u is the control, w is the exogenous input, k is the timestep number, Δt is the timestep length, J is the cost, and N is the final timestep number.

Depending on the problem discretization, hundreds of thousands of calculations may be required to determine the globally optimal control through DP and typically a low-fidelity, low computational cost vehicle model is needed. Numerous low computational cost vehicle models have been employed in research, and thorough descriptions of model development are available in the literature [76, 77].

To implement an Optimal EMS in a 2012 Toyota Prius PHEV, an approximate model of a power-split PHEV is required (shown in Fig. 5). The model consists of a force balance in the longitudinal direction to capture vehicle dynamics, a propulsion

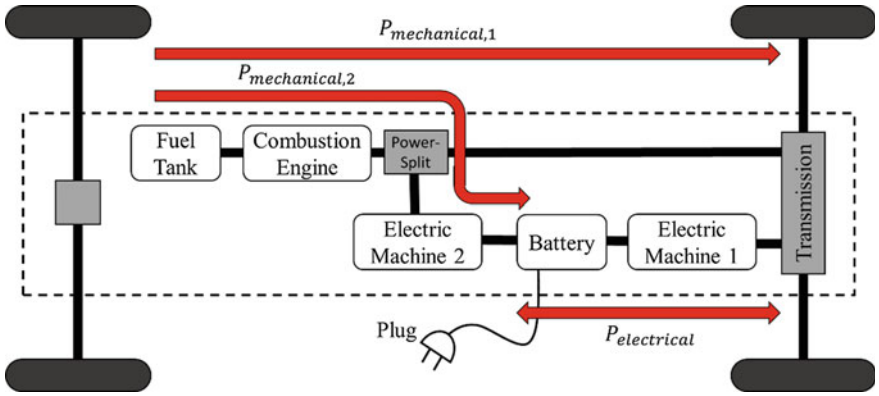

Fig. 5 A power-split PHEV schematic showing operation in parallel mode (propulsion power from mechanical, electric, or both) and series mode (propulsion power from the engine stored in the battery)

equation accounting for energy conversion efficiencies, a lithium-ion battery model, a brake-specific fuel consumption engine map (typically approximated with a response surface), and drivetrain torque and speed constraint equations all using appropriate vehicle parameters. A comprehensive derivation of the low computational cost vehicle model is available in a previous publication from our research group [5].

For a PHEV Optimal EMS DP derivation, the state is chosen to be the SOC, the control is chosen to be the engine power (P_{ICE}), the exogenous input is the vehicle (v), and the cost is chosen to be the fuel mass required (m_{fuel}). This formulation with the added feasibility constraints for a PHEV yields the following modified equations:

$$\mathrm{SOC}(k+1) = \mathrm{SOC}(k) + f(\mathrm{SOC}, P_{\mathrm{ICE}}, v, k)\Delta t \tag{5}$$

$$\mathrm{Cost} = \sum_{k=0}^{N-1} f(\mathrm{SOC}, P_{\mathrm{ICE}}, v, k, \Delta t) \tag{6}$$

$$\mathrm{SOC}_{\min} \leq \mathrm{SOC}(k) \leq \mathrm{SOC}_{\max} \quad (k = 0, \ldots N) \tag{7}$$

$$P_{\mathrm{ICE,min}} \leq P_{\mathrm{ICE}}(k) \leq P_{\mathrm{ICE,max}} \quad (k = 0, \ldots N-1) \tag{8}$$

A timestep of $\Delta t = 1$ s and a discretization of $\Delta\mathrm{SOC} = 0.02\%$ $\Delta P_{\mathrm{ICE}} = 0.1$ kW were chosen, and the resulting control map solution is incorporated into the high-fidelity Autonomie simulation using a 2-D lookup table Simulink block.

Note: The initial SOC value is chosen to be 23% with a charge sustaining value of 20%. This ensures there will be a surplus of battery power to be used while also

ensuring that engine power must be used for all drive cycles investigated. FE will be improved by using all excess battery power (ending the drive cycle at 20% SOC) while using engine power only when necessary.

4.2 Optimal EMS Results

When comparing the desired engine power of the Baseline EMS to the desired engine power of the Optimal EMS (shown in Fig. 6), it is apparent that for each of the drive cycles, an engine power around 20 kW is often optimally efficient. However, an application of 20 kW of engine power is only efficient at certain speeds, which are known to the Optimal EMS from drive cycle prediction.

When comparing the battery SOC from the Baseline EMS and the Optimal EMS (Fig. 7), it is apparent that the Optimal EMS ends the drive cycle at the minimum allowable value. Since the Baseline EMS does not use drive cycle end information, it is at a significant disadvantage.

FE improvements are shown in Fig. 8 and are calculated as

$$\text{FE Improvement} = \frac{\text{New FE} - \text{Baseline FE}}{\text{Baseline FE}} \tag{9}$$

An Optimal EMS provided the largest FE increase in city drive cycles (UDDS and NYCC) which have frequent accelerations and decelerations. For aggressive

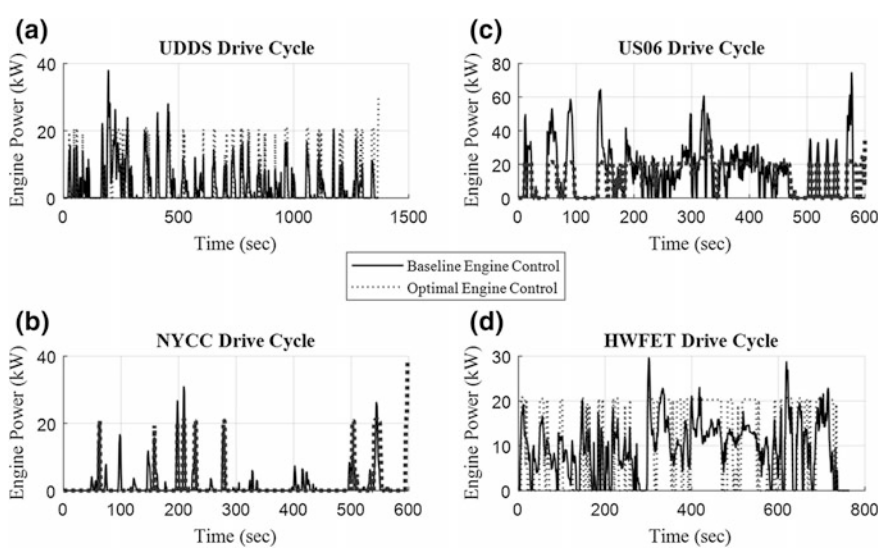

Fig. 6 A comparison of the engine power used by the Baseline EMS and the engine power used by the Optimal EMS

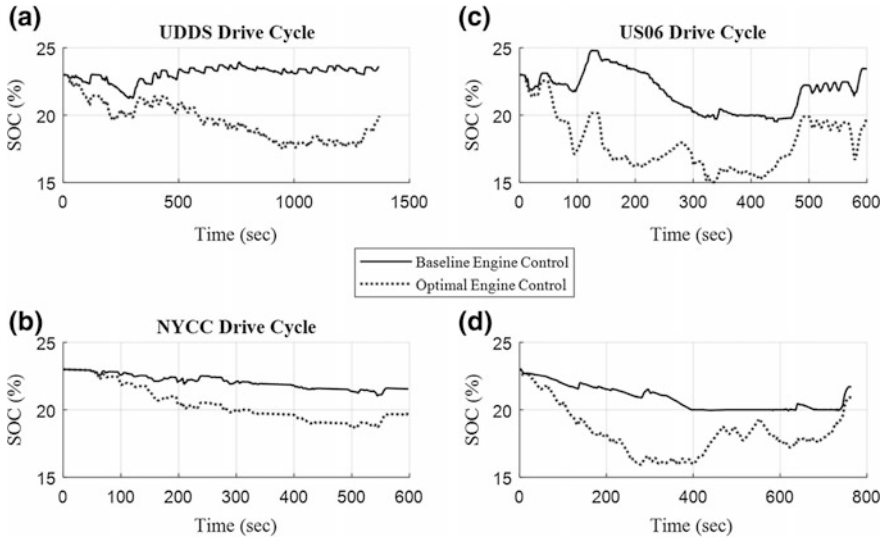

Fig. 7 A comparison of the battery SOC results from the Baseline EMS and the battery SOC results from the Optimal EMS

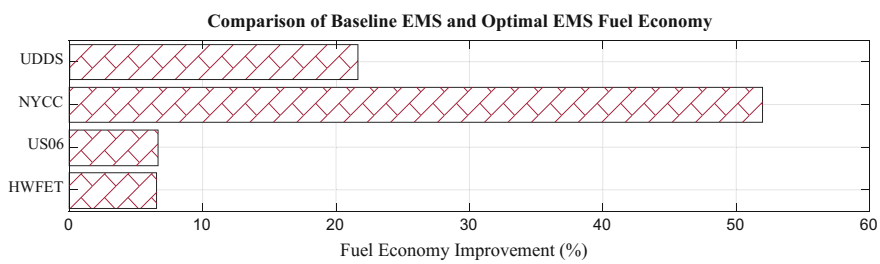

Fig. 8 A comparison of the Baseline EMS fuel economy results and the Optimal EMS fuel economy results

and highway drive cycles, there is less freedom in powertrain operation due to high power demand, resulting in less dramatic FE improvements.

5 Planning Method 2: Eco-Driving

Eco-Driving enables FE improvements by modifying vehicle speed along a fixed drive cycle. Eco-Driving can be communicated and encouraged to the driver in a variety of ways including driver training, vehicle dashboards, smartphone applications, and pedal feedback [78] (examples shown in Fig. 9).

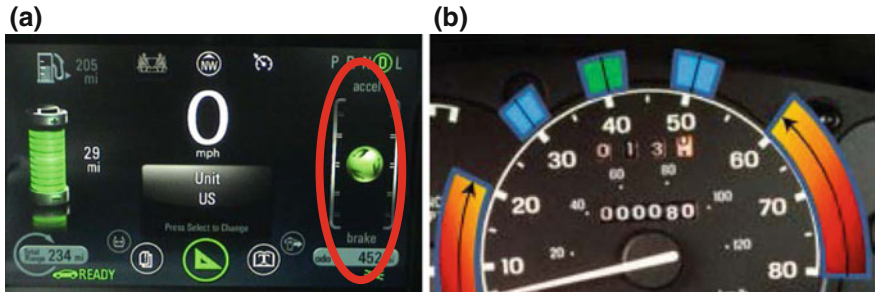

Fig. 9 Eco-Driving achieves a FE improvement through lower energy driving which is encouraged by driver feedback. An existing implementation of this feedback from a 2012 Chevrolet Volt dashboard is shown (**a**) as well as a proposed general advice image from the literature [79] (**b**)

Eco-Driving can be formulated using an optimal control approach as

$$\min: \quad P_{\text{prop}}(k) \tag{10}$$

$$\text{subject to}: \quad \text{time constraints (e.g.} \quad t_{\text{total}} \leq t_{\max}) \tag{11}$$

$$\text{safety constraints (e.g.} \quad v \leq v_{\text{speed limit}}) \tag{12}$$

$$\text{operational constraints (e.g.} \quad a \leq a_{\text{limit}}) \tag{13}$$

However, in this formulation, it can be difficult to incorporate real-world constraints such as traffic lights, other vehicles, and pedestrians. Because of this difficulty, rules have been extracted from studying the results of optimal control problems. The rules are typically generalized as eliminating full stops, maintaining a constant speed, limiting acceleration, and smoothing the velocity profile [78–82]. Each of these rules will be examined independently by eliminating stops in the UDDS drive cycle, maintaining a more constant speed in the NYCC drive cycle, limiting acceleration and deceleration in the US06 drive cycle, and smoothing the velocity in the HWFET drive cycle. The FE results will not be as drastic as when all methods are combined, but instead will shed light on the relative importance of each rule.

5.1 Deriving Eco-Driving Strategies

To study the effect of removed stops from drive cycles, the UDDS drive cycle was modified by removing velocities below 15 mph while preserving the overall drive cycle distance. This modified drive cycle is compared to the original as shown in Fig. 10a. Note that in Fig. 10b, the acceleration magnitudes remain approximately

the same except for a few reductions. The engine power also remains relatively unaffected as shown in Fig. 10c, and the battery SOC has a similar profile but ends at a higher value of SOC.

To study the effect of a more constant velocity, the NYCC drive cycle was modified by increasing the speed in some sections and reducing speeds in other sections while preserving the overall drive cycle distance. This modified drive cycle is compared to the original in Fig. 11a. These modifications significantly affect the acceleration, as shown in Fig. 11b, but the reductions in acceleration contribute to the improved performance. Figure 11c shows a drastically different engine power used by the Baseline EMS for the modified NYCC drive cycle. Engine power is increased in some areas and decreased in other areas. Figure 11d shows that the SOC ends at a significantly higher value, which is not ideal for a PHEV seeking to end the drive cycle at the lowest possible value of battery SOC.

To lower the propulsive power required in aggressive driving, the acceleration and deceleration magnitudes can be reduced. To study this effect, the US06 aggressive drive cycle was modified by limiting the acceleration magnitude to below 1.5 m/s^2 and above the deceleration rate of −1.5 m/s^2 while preserving the overall drive cycle distance, which is shown in Fig. 12b. Reducing acceleration magnitudes has the favorable effect of reducing peak engine power (Fig. 12c). Figure 12d shows a smoother SOC profile resulting from the reduced acceleration magnitudes.

To study the effect of velocity smoothing, the HWFET drive cycle can be modified by aggressively smoothing the velocity profile while preserving the overall drive cycle distance. This modified drive cycle is compared to the original as shown in Fig. 13a. This drive cycle modification has a drastic effect on the drive

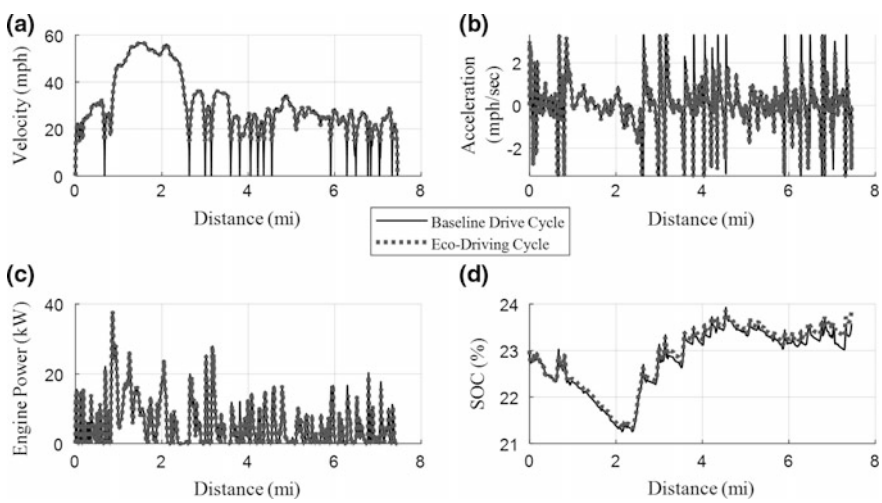

Fig. 10 A comparison of the changes that occur along the drive cycle and in vehicle operation when removing stop and go driving from the UDDS drive cycle

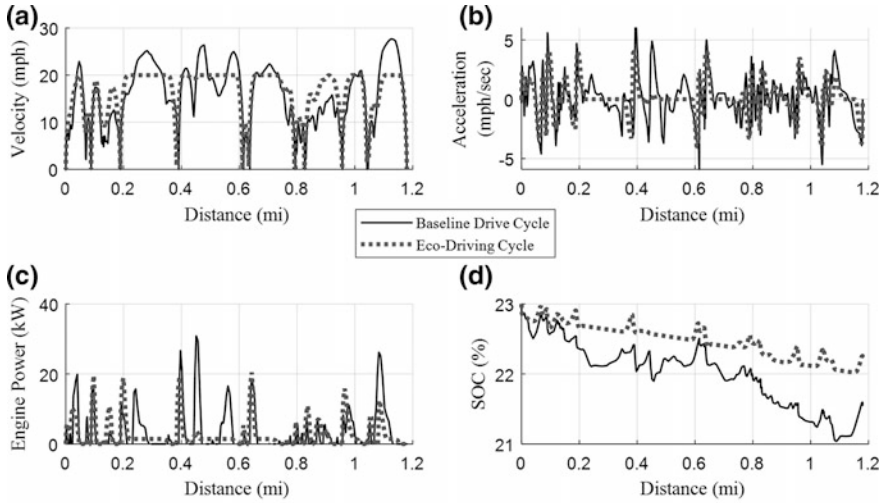

Fig. 11 A comparison of the changes that occur along the drive cycle and in vehicle operation when making vehicle speed more consistent along the NYCC drive cycle

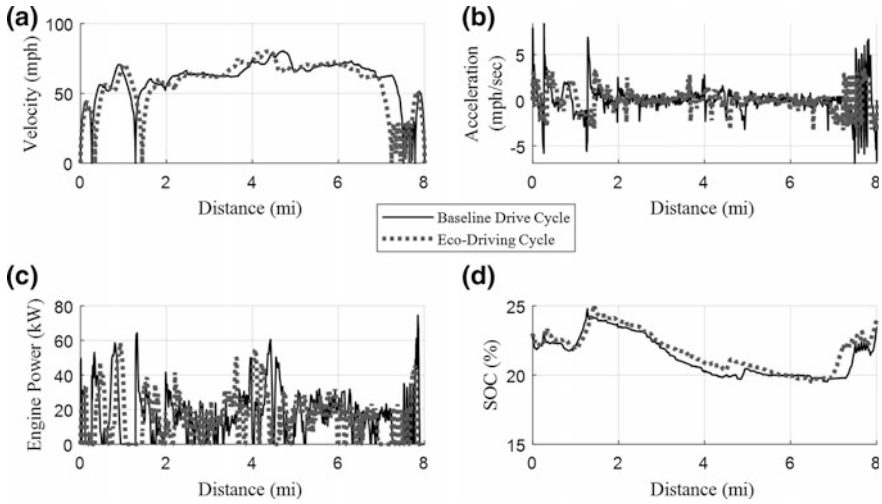

Fig. 12 A comparison of the changes that occur along the drive cycle and in vehicle operation when limiting acceleration and deceleration rates along the US06 drive cycle

cycle acceleration as shown in Fig. 13b. For much of the drive cycle, the acceleration magnitude is almost completely eliminated. When the drive cycle is smoothed, the engine operation is also smoothed as shown in Fig. 13c, although the overall shape of engine power remains consistent. Also, by smoothing the drive cycle, the battery SOC remains consistent as shown in Fig. 13d.

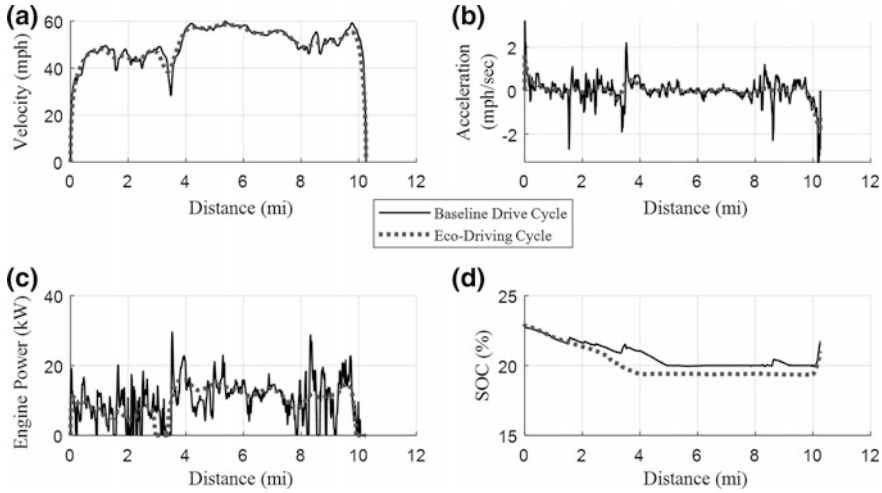

Fig. 13 A comparison of the changes that occur along the drive cycle and in vehicle operation when smoothing the drive cycle velocity along the HWFET drive cycle

5.2 *Eco-Driving Results*

Figure 14 demonstrates that significant FE improvements can be realized by eliminating stops and by reducing acceleration/deceleration magnitudes, both of which reduce the total energy expended during the drive cycle. Driving at a more constant speed, as demonstrated in the NYCC drive cycle, can provide moderate FE improvements, while smoothing the velocity profile provides a small FE improvement.

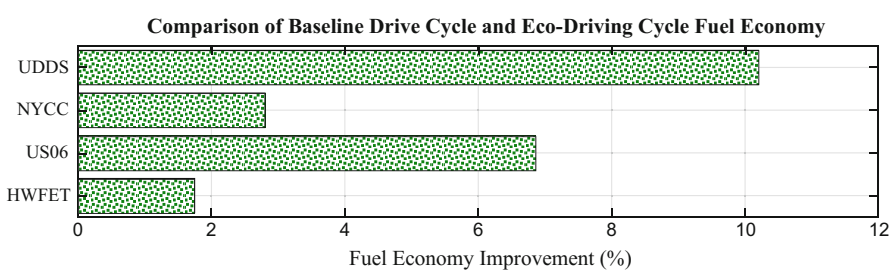

Fig. 14 Fuel economy results for removing stops along the UDDS drive cycle, creating a more constant speed along the NYCC drive cycle, limiting acceleration and deceleration rates along the US06 drive cycle, and smoothing the velocity profile for the HWFET drive cycle

6 Planning Method 3: Eco-Driving and an Optimal Energy Management Strategy

Combining Eco-Driving with an Optimal EMS has received little attention in the literature, but could result in FE increases beyond what is possible from either strategy alone. Removing drive cycle power restrictions through Eco-Driving provides an Optimal EMS with even greater freedom for FE improvements.

6.1 Eco-Driving and an Optimal EMS Results

For the Eco-Driving drive cycles, as with the baseline drive cycles, the Optimal EMS most often seeks an engine power of approximately 20 kW. In the UDDS and US06 drive cycles, significant engine power reductions are achieved, while in the NYCC and HWFET drive cycles, significant engine power increases are achieved as shown in Fig. 15.

Knowledge of the entire drive cycle in advance allows a final battery SOC of 20% to be achieved for all drive cycles. Since there is no adjusted FE penalty that must be calculated for PHEVs since they are designed to end at the minimum SOC, this provides a significant FE benefit. Note that in the highway drive cycle, there is significantly more SOC fluctuation from only running the engine at 20 kW.

The FE improvements from Eco-Driving combined with an Optimal EMS are significant. For the NYCC drive cycle, the regions of constant vehicle speed

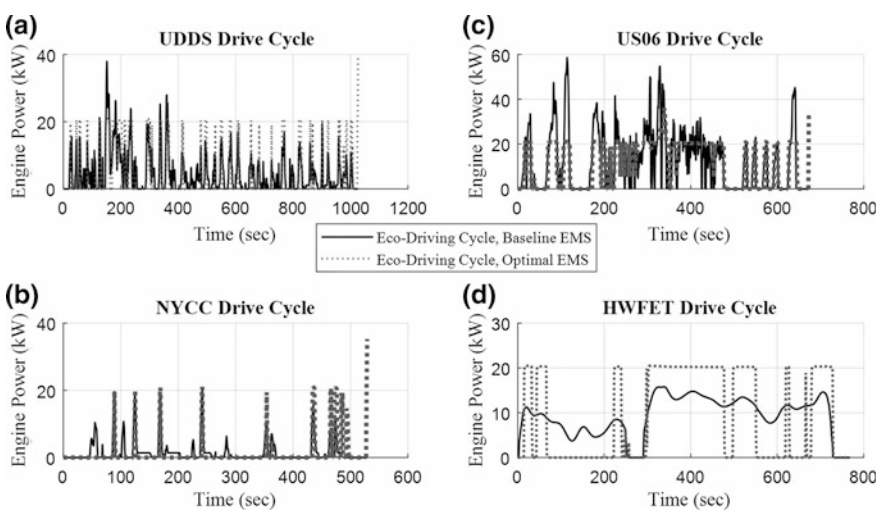

Fig. 15 A comparison of the engine power used by the Baseline EMS along the Eco-Driving drive cycle and the engine power used by the Optimal EMS along the Eco-Driving drive cycle

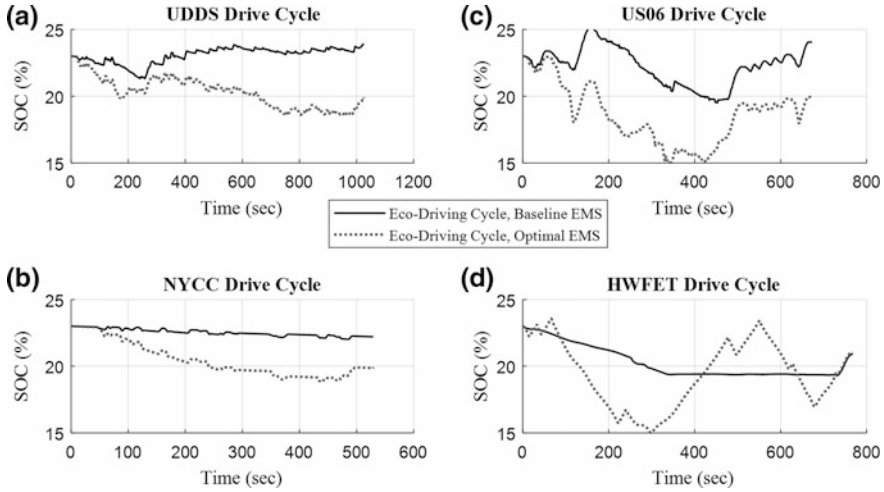

Fig. 16 Battery SOC for **a** UDDS, **b** NYCC, **c** US06, and **d** HWFET

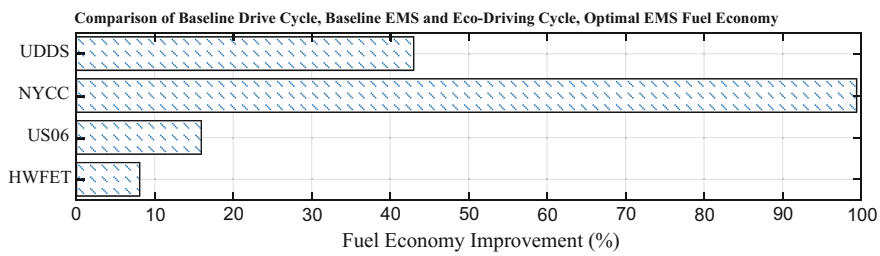

Fig. 17 Fuel economy results for various aspects of Eco-Driving combined with an Optimal EMS along the UDDS, NYCC, US06, and HWFET drive cycles

provided from Eco-Driving allow the Optimal EMS to achieve high powertrain efficiency and realize significant FE benefits. Additionally, knowledge of the drive cycle allows perfect utilization of battery energy, which is lost from Eco-Driving alone (Fig. 16b). A similar phenomenon is observed for the UDDS and US06 drive cycles. Conversely, the HWFET drive cycle realized a FE benefit but at the expense of wild battery SOC fluctuations which may impact battery life (Fig. 17).

6.2 Comparing Planning Strategies

When comparing all three vehicle control strategies enabled by connected and autonomous lithium-ion electric vehicles, it is apparent (from Fig. 18) that the largest FE improvements are possible when combining Eco-Driving with an

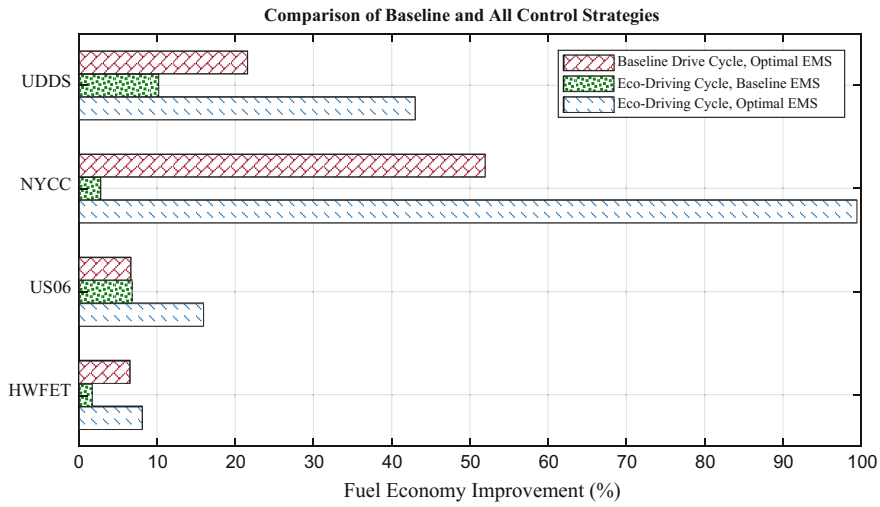

Fig. 18 FE results comparing the FE improvements from a baseline drive cycle with a Baseline EMS to: (top bar) a baseline drive cycle with an Optimal EMS, (middle bar) an Eco-Driving drive cycle, with a Baseline EMS, and (bottom bar) an Eco-Driving drive cycle with an Optimal EMS

Optimal EMS while the next largest FE improvements are achieved using the Optimal EMS on the baseline drive cycle. Note that the Eco-Driving FE improvements are from individual investigation of Eco-Driving rules, and if all rules were to be combined, the Eco-Driving FE improvement would be more significant. Additionally, city drive cycles with velocities modified to be consistent speeds or with stop elimination provide large FE improvements from an Optimal EMS. Limiting acceleration and deceleration rates in aggressive drive cycles provides double the FE improvement from an Optimal EMS. Smoothing vehicle velocity during highway drive cycles provides a marginal FE improvement increase from an Optimal EMS.

7 Conclusions

When CAV technologies are combined with lithium-ion electric vehicle technology, new vehicle control strategies that improve FE are possible. In this chapter, a review of CAV technologies, lithium-ion electric vehicle modeling techniques, and three control strategies for improved FE were presented. The results demonstrate that significant FE gains can be achieved through the realization of an Optimal EMS, Eco-Driving, and from the combination of an Optimal EMS and Eco-Driving.

Although there are several CAV technologies that are not currently available, it may be possible to achieve significant portions of these FE benefits today. As more vehicles incorporate electrification and CAV technologies, these FE improvements will be easier to achieve, thus helping to achieve transportation sustainability.

References

1. *Annual Energy Outlook 2017*. Energy Information Administration (5 Jan 2017) AEO2017
2. Z.D. Asher, V. Wifvat, A. Navarro, S. Samuelsen, T.H. Bradley, SAE Technical Paper 2017-26-0106 (2017), https://doi.org/10.4271/2017-26-0106
3. D.J. Fagnant, K. Kockelman, Transp. Res. A Policy **77**, 167–181 (2015)
4. M. Broussely, in *Electric and Hybrid Vehicles: Power Sources, Models, Sustainability, Infrastructure and the Market*, ed. by G. Pistoia (Elsevier, Amsterdam, 2010), pp. 305–347
5. Z.D. Asher, D.A. Baker, T.H. Bradley, IEEE Trans. Control Syst. Tech. PP **99**, 1–14 (2017). https://doi.org/10.1109/tcst.2017.2747502
6. A. Iliaifar, LIDAR, lasers, and logic: anatomy of an autonomous vehicle (2013), www.digitaltrends.com
7. M. Trimarchi, *Do Car GPS Devices Cause Accidents*? (Howstuffworks.com., Atlanta, 2017)
8. M. Bertozzi, A. Broggi, A. Fascioli, Rob. Auton. Syst. **32**, 1–16 (2000)
9. Z. Sun, G. Bebis, R. Miller, IEEE Trans. Pattern Anal. Mach. Intell. **28**, 694–711 (2006)
10. A. Ruta, F. Porikli, S. Watanabe, Y. Li, Mach. Vis. Appl. **22**, 359–375 (2011)
11. F. Lindner, U. Kressel, S. Kaelberer, Robust recognition of traffic signals. IEEE Intell. Veh. Symp. 49–53 (2004)
12. M.A.S. Kamal, M. Mukai, J. Murata, T. Kawabe, IEEE Trans. Intell. Transp. Syst. **4**, 244–251 (2010)
13. M. Munoz-Organero, V.C. Magana, IEEE Trans. Intell. Transp. Syst. **14**, 1023–1028 (2013)
14. E. Ohn-Bar, A. Tawari, S. Martin, M.M. Trivedi, Comput. Vis. Image Underst. **134**, 130–140 (2015)
15. E. Raphael, R. Kiefer, P. Reisman, G. Hayon, SAE Int. J. Passeng. Cars Mech. Syst. **4**, 467–478 (2011)
16. M.M. Trivedi, T. Gandhi, J. McCall, IEEE Trans. Intell. Transp. Syst. **8**, 108–120 (2007)
17. E. Dagan, O. Mano, G.P. Stein, A. Shashua, Forward collision warning with a single camera. IEEE Intell. Veh. Symp. Proc. 37–42 (2004)
18. G.P. Stein, O. Mano, A. Shashua, Vision-based ACC with a single camera: bounds on range and range rate accuracy. IEEE Intell. Veh. Symp. Proc. 120–125 (2003)
19. S. Clark, H. Durrant-Whyte, Autonomous land vehicle navigation using millimeter wave radar, in *Proceedings 1998 IEEE International Conference on Robotics and Automation (Cat. No. 98CH36146)*, vol. 4, May 1998, pp. 3697–3702
20. D.J. Belgiovane, C.C. Chen, S.Y.P. Chien, R. Sherony, IEEE Trans. Intell. Transp. Syst. **99**, 1–10 (2017). http://ieeexplore.ieee.org
21. Z. Ji, M. Luciw, J. Weng, S. Zeng, IEEE Trans. Intell. Transp. Syst. **12**, 402–411 (2011)
22. B. Steux, C. Laurgeau, L. Salesse, D. Wautier, Fade: a vehicle detection and tracking system featuring monocular color vision and radar data fusion. IEEE Intell. Veh. Symp. Proc. **2**, 632–639 (2002)
23. A. Gern, U. Franke, P. Levi, Robust vehicle tracking fusing radar and vision, in IEEE *International Conference on Multisensor Fusion and Integration* for *Intelligent Systems (MFI'01)* (2001) pp. 323–328
24. P. Themann, T. Uhrner, D. Kuck, M. Müller, M. Klubal, Ecodriving support based on cooperative prediction models, in *19th ITS World Congress* (Vienna, Austria, 2012), pp. 22–26

25. F. Mensing, E. Bideaux, R. Trigui, H. Tattegrain, Transp. Res. Part D Transp. Environ. **18**, 55–61 (2013)
26. S. Tokoro, K. Kuroda, A. Kawakubo, K. Fujita, H. Fujinami, Electronically scanned millimeter-wave radar for pre-crash safety and adaptive cruise control system. IEEE Intell. Veh. Symp. Proc. 304–309 (2003)
27. G.R. Widmann et al., SAE Technical Paper Series, No. 724 (2000)
28. F. Rahman, C. O'Brien, K. Manning, Let EcoDrive be your guide: development of a mobile tool to reduce carbon footprint and promote green transport, in *Proceedings of the 27th Annual ACM Symposium on Applied Computing* (2012), pp. 519–524
29. K. Jakobsen, S.C.H. Mouritsen, K. Torp, Evaluating eco-driving advice using gps/canbus data, in *21st ACM SIGSPATIAL International Conference on Advances in Geographic Information Systems SIGSPATIAL'13* (2013), pp. 44–53
30. D.A. Baker, Z.D. Asher, T.H. Bradley, SAE Technical Paper (2017), http://papers.sae.org/2017-01-1262/, https://doi.org/10.4271/2017-01-1262
31. F.A. Bender, M. Kaszynski, O. Sawodny, IEEE Trans. Veh. Tech. **62**(8), 3581–3592 (2013). http://ieeexplore.ieee.org
32. A.G. Adinolfi, H.K. Kuga, M.L. de Oliveira e Souza, SAE Technical Paper 2013-36-0650 (2013)
33. Z. Popovic, A. Soloviev, Y. Mochizuki, SAE Technical Paper 2011-01-1035 (2011)
34. Z. Popovic Y. Mochizuki, SAE Technical Paper 2011-01-1036 (2011)
35. H. Kitano, H. Kazuo, H. Tanaka, An estimation method of vehicle position for automated driving with GNSS, in *SAE World Congress and Exhibition* (2016)
36. E. Stenborg, L. Hammarstrand, Using a single band GNSS receiver to improve relative positioning in autonomous cars, in *Intelligent Vehicles Symposium* (2016)
37. F. Meng, S. Tan, S. Wang, B. Zhu, New techniques to enhance the performance of stand-alone GNSS positioning. in *International Conference on Communication and Networks* (2015), pp. 548–552
38. M. Campbell, M. Egerstedt, J.P. How, R.M. Murray, Phil. Trans. Series A Math. Phys. Eng. Sci. 368 (1928), 4649–4672 (2010). http://rsta.royalsocietypublishing.org
39. C. Sun, S.J. Moura, X. Hu, J.K. Hedrick, F. Sun, IEEE Trans. Control Syst. Tech. 23(3), 1075–1086 (2015). http://ieeexplore.ieee.org
40. C. Sun, F. Sun, H. He, App. Energy **185**, 1644–1653 (2017)
41. C. Smith, *The Car Hacker's Handbook: A Guide for the Penetration Tester* (No Starch Press, Inc., San Fransico, 2016)
42. M. Kerper, C. Wewetzer, H. Trompeter, W. Kiess, M. Mauve, Driving more efficiently—The use of inter-vehicle communication to predict a future velocity profile, in *IEEE Vehicular Technology Conference* (2011), pp. 1–5
43. D. Lang, R. Schmied, L. Del Re, SAE Int **7**, 14 (2014)
44. M.A. Mohd Zulkefli, J. Zheng, Z. Sun, H.X. Liu, Transp. Res. Part C Emerg. Technol. **45**, 41–63 (2014)
45. M. Brackstone, M. McDonald, Transp. Res. Part F Traffic Psychol. Behav. **2**, 181–196 (1999)
46. B. Asadi, A. Vahidi, in *IFAC Proceedings Volumes* **42**(15), 484–489 (2009)
47. B. Asadi, A. Vahidi, IEEE Trans. Control Syst. Technol. **19**, 707–714 (2011)
48. S. Mandava, K. Boriboonsomsin, M. Barth, Arterial velocity planning based on traffic signal information under light traffic conditions, in *Proceedings of IEEE Conference* on *Intelligent Transportation Systems* (ITSC) (2009), pp. 1–6
49. E. Koenders, J. Vreeswijk, Cooperative infrastructure, in *IEEE Intelligent Vehicles Symposium, Proceedings* (2008), pp. 721–726
50. Q. Gong, Y. Li, Z.R. Peng, IEEE Trans. Veh. Tech. **57**, 3393–3401 (2008)
51. Q. Gong, Y. Li, Z. Peng, Power Management of plug-in hybrid electric vehicles using neural network based trip modeling, in *American Control Conference* (2009), pp. 4601–4606. http://ieeexplore.ieee.org

52. J. Gonder, A. Brooker, E. Burton, L. Wang, E. Wood, Mobility patterns informing V2X research projects: eco-routing and electrified roadway project examples, in *Task 28 Workshop, Home Grids and V2X Technologies* (2016)
53. S.E. Li, S. Xu, X. Huang, B. Cheng, H. Peng, IEEE Trans. Veh. Technol. **64**, 5439–5449 (2015)
54. T. Edwards, IEEE Intell. Transp. Syst. Mag. **7**, 4 (2015)
55. D. Krajzewicz, M. Heinrich, M. Milano, COLOMBO: investigating the potential of V2X for traffic management purposes assuming low penetration rates, in *9th ITS European Congress*, Dublin (IE), 4–7 June 2013
56. Y. Chen, D. Zhang, K. Li, Enhanced eco-driving system based on V2X communication, in *Proceedings of IEEE Conference on Intelligent Transportation Systems (ITSC)* (2012), pp. 200–205
57. S. Diewald, A. Möller, L. Roalter, M. Kranz, in *Proceedings of Mensch und Computer*, Konstanz, Germany, 1–8 Sept 2012
58. C. Weiß, Comput. Netw. **55**, 3103–3119 (2011)
59. B. Schünemann, J.W. Wedel, I. Radusch, Tamkang. J. Sci. Eng. **13**, 637–641 (2010)
60. N. Kim, M. Duoba, A. Rousseau, SAE Int. **6**, 985–992 (2013). https://doi.org/10.4271/2013-01-1458
61. N. Kim, A. Rousseau, E. Rask, SAE Int **2012**, 1–14 (2012). https://doi.org/10.4271/2012-01-1040
62. P. Fritzson, P. Aronsson, H. Lundvall, K. Nyström, A. Pop, L. Saldamli, D. Broman, The OpenModelica modeling, simulation, and development environment, in *Conference on Simulation and Modelling of the Scandinavian Simulation Society (SIMS2005)* (Trondheim, Norway, 2005)
63. H. Tummescheit. Ph.D. dissertation, Lund University (2002)
64. B.M. Geller, T.H. Bradley, SAE Technical Paper (2011). https://doi.org/10.4271/2011-01-0943
65. Argonne National Lab, Downloadable dynamometer database (D3)—Test 37; summary sheet. PHEV 2012 Toyota Prius, 72°F. https://www.anl.gov/energy-systems/group/downloadable-dynamometer-database/plug-hybrid-electric-vehicles/2012-toyota
66. C. Lin, J. Kang, J.W. Grizzle, H. Peng, Energy management strategy for a parallel hybrid electric truck, in *American Control Conference (Cat. No. 01CH37148)*, vol. 4 (2001), pp. 2878–83. http://ieeexplore.ieee.org
67. R. Bellman, Dynamic programming and lagrange multipliers. Proc. Natl. Acad. Sci. USA, **42**(10), Nat. Acad Sci. **76** (1956)
68. N. Kim, S. Cha, H. Peng, IEEE Trans. Control Syst. Technol. **19**, 1279–1287 (2011)
69. V.G. Boltyanskii, R.V. Gamkrelidze, L.S. Pontryagin, *The Theory of Optimal Processes. I. The Maximum Principle* (TRW Space Technology Laboratories, Los Angeles, California, 1960). http://www.dtic.mil/docs/citations/AD0264147
70. C. Lin, H. Peng, J.W. Grizzle, A stochastic control strategy for hybrid electric vehicles, in *American Control Conference*, vol. 5 (2004), pp. 4710–4715. http://ieeexplore.ieee.org
71. S. Onori, L. Serrao, G. Rizzoni, Adaptive equivalent consumption minimization strategy for hybrid electric vehicles, in *2010 ASME Dynamic Systems and Control Conference*, vol. 499 (American Society of Mechanical Engineers, 2010)
72. D. Bianchi, L. Rolando, L. Serrao, S. Onori, G. Rizzoni, N. Al-Khayat, T. Hsieh, P. Kang, A rule-based strategy for a series/parallel hybrid electric vehicle: an approach based on dynamic programming, in *ASME 2010 Dynamic Systems* and *Control Conference,* vol. 507 (American Society of Mechanical Engineers, 2010)
73. G. Paganelli, S. Delprat, T.M. Guerra, J. Rimaux, J.J. Santin, Equivalent consumption minimization strategy for parallel hybrid powertrains, in *IEEE Vehicular Technology Conference VTC Spring 2002 (Cat. No. 02CH37367)*, vol. 4 (2002), pp. 2076–2081. http://ieeexplore.ieee.org

74. H.A. Borhan, A. Vahidi, A.M. Phillips, M. L. Kuang, I.V. Kolmanovsky, Predictive energy management of a power-split hybrid electric vehicle, in *American Control Conference* (2009), pp. 3970–3976. http://ieeexplore.ieee.org
75. P. Zhang, F. Yan, C. Du, 2015/8. Renew. Sust. Energy Rev. **48**, 88–104 (2015)
76. I. Husain, *Electric and Hybrid Vehicles: Design Fundamentals*, 2nd edn. (CRC Press, Boca Raton, 2010)
77. R. Rajamani, *Vehicle Dynamics and Control*, 2nd edn. (Springer, New York, 2011)
78. J. Gonder, M. Earleywine, W. Sparks SAE Int. J. Passeng. Cars Electron Electr. Syst. **5**, 450–461 (2012-01-0494) (2012). http://papers.sae.org
79. P. Michel, D. Karbowski, A. Rousseau, SAE Technical Paper (2016). http://papers.sae.org/2016-01-0152/
80. Y. Saboohi, H. Farzaneh, App. Energy **86**, 1925–1932 (2009)
81. S. Mandava, K. Boriboonsomsin, M. Barth, arterial velocity planning based on traffic signal information under light traffic conditions. IEEE Intell. Trans. Syst. 1–6 (2009). http://ieeexplore.ieee.org
82. D. Wissam, A. Chasse, A. Sciarretta, P. Moulin, Optimal energy management compliant with online requirements for an electric vehicle in eco-driving, in *Workshop on Engine and Powertrain Control, Simulation and Modeling*, Rueil-Malmaison, France, Oct 2012